Experimental determination of intrinsic parameters in double-donor-doped $(Ba_{0.92}Sr_{0.08})TiO_3$-based positive temperature coefficient ceramics

2004 J. Phys.: Condens. Matter 16 6961

(http://iopscience.iop.org/0953-8984/16/39/028)

INSTITUTE OF PHYSICS PUBLISHING JOURNAL OF PHYSICS: CONDENSED MATTER

J. Phys.: Condens. Matter **16** (2004) 6961–6968 PII: S0953-8984(04)78885-2

Experimental determination of intrinsic parameters in double-donor-doped $(Ba_{0.92}Sr_{0.08})TiO_3$-based positive temperature coefficient ceramics

Zeming He[1], J Ma[1], Yuanfang Qu[2] and Xuemei Feng[2]

[1] School of Materials Engineering, Nanyang Technological University, Nanyang Avenue, Singapore 639798, Singapore
[2] Materials Institute, Tianjin University, Tianjin 300072, Tianjin, People's Republic of China

E-mail: zmhe@ntu.edu.sg

Received 1 April 2004, in final form 4 August 2004
Published 17 September 2004
Online at stacks.iop.org/JPhysCM/16/6961
doi:10.1088/0953-8984/16/39/028

Abstract

In the present work, double-donor-doped $(Ba_{0.92}Sr_{0.08})TiO_3$-based positive temperature coefficient (PTC) ceramics were fabricated for potential application in an over-current protector. The electrical properties of the materials were also characterized. Using the experimental results obtained, theoretical models on electrical properties were studied, and the intrinsic parameters were determined. The relationship between the intrinsic parameters, the materials variables and the electrical properties was discussed. It was noted that the addition of double donors $Y_2O_3 + Nb_2O_5$ could result in relatively low room-temperature resistivity, in particular, 30 Ω cm at the sintering temperature of 1230 °C. Within the investigated working temperature range, the grain-boundary potential barrier at a fixed measuring temperature decreased with increasing sample sintering temperature. The evaluated effective donor concentration and surface acceptor state density were in good agreement with the reported values in the literature. A parameter was introduced based on these two variables to represent the resistivity jump. The depletion layer thickness was determined to be in the submicron range. The present work is believed to be the first report to determine, based on the experimental data, all the essential intrinsic parameters for double-donor-doped PTC ceramics.

1. Introduction

Donor-doped barium titanate can be semiconductive and its electrical resistance exhibits a positive temperature coefficient (PTC) effect [1]. This anomalous phenomenon has been explained [2–6], and the models proposed by Heywang [2] and Jonker [3] are most widely

accepted. In materials, the PTC effect originates from the presence of grain-boundary depletion layers, which consist of two dimensional surface acceptor states. The surface states take up neighbouring conduction electrons, which gives rise to negatively charged boundary layers followed by positive space charges at both sides, forming grain-boundary potential barriers for the remaining conduction electrons. At temperatures below the Curie point, the potential barrier could be compensated by the charges arising from the ferroelectric spontaneous polarization. When the temperature rises above the Curie temperature, the spontaneous polarization disappears and the potential barrier restores, leading to a resistivity jump.

Taking advantage of their electrical properties, PTC components have been extensively used in various fields such as over-current protectors, self-regulating heaters, or temperature sensors [7]. Recently, a PTC over-current protector has attracted even more attention due to the increasing demand on the safety and reliability of products. However, challenges still exist in these applications, especially in microelectronic circuits working at low voltage, where the relatively high room-temperature resistivity results in application restriction [8].

In the present work, $(Ba_{0.92}Sr_{0.08})TiO_3$-based PTC ceramics were fabricated by doping $Y_2O_3 + Nb_2O_5$ double donors, in an attempt to reduce the material's room-temperature resistivity. The correlation of the sintering temperature with the electrical properties is discussed. Based on the theoretical models [2, 3] and the experimental results obtained, the intrinsic parameters, such as grain-boundary potential barrier, effective donor concentration and surface acceptor state density, are determined and discussed. The relationship between the intrinsic parameters and the composition and processing and hence the apparent electrical properties is interpreted.

2. Theoretical models

For PTC ceramics, the depletion layer thickness b of the grain-boundary potential barrier is expressed as

$$b = \frac{N_s}{N_d} \tag{1}$$

where N_s is the density of the surface acceptor state at the grain boundary and N_d is the effective donor concentration within the grain. The effective donor concentration is

$$N_d = \frac{1}{\rho_b e \mu} \tag{2}$$

where ρ_b is the grain resistivity extracted from the high frequency intercept in the complex impedance diagram, and e and μ are electron charge and mobility, respectively.

Above the Curie temperature, the resistivity ρ is related to the grain-boundary potential barrier ϕ as

$$\rho = \rho_0 \exp\left(\frac{e\phi}{kT}\right) \tag{3}$$

where ρ_0 is a constant, and k and T are the Boltzmann constant and the absolute temperature, respectively. The detailed expression of the potential barrier is

$$\phi = \frac{eN_s^2}{2\varepsilon_0 \varepsilon_r N_d} \tag{4}$$

where ε_0 is the free-space permittivity and ε_r is the relative permittivity of the material. The relative permittivity above Curie temperature is described by the Curie–Weiss law as

$$\varepsilon_r = \frac{C}{T - T_C} \tag{5}$$

where C is the Curie constant and T_C is the absolute Curie temperature.

3. Experimental procedure

The raw materials were commercially available reagent-grade powders. $BaCO_3$, $SrCO_3$ and TiO_2 were used to form the principal crystalline phase of (Ba, Sr)TiO_3. Y_2O_3, Nb_2O_5, MnO_2, Al_2O_3, SiO_2, TiO_2 and BN were used as the additives for property modification.

The composition designed in the present work was $(Ba_{0.92}Sr_{0.08})TiO_3 + 0.0010Y_2O_3 + 0.0005Nb_2O_5 + 0.0004MnO_2 + 0.1AST + 0.02BN$, where AST indicates a mixture of Al_2O_3, SiO_2 and TiO_2. The weighted powders for the composition were mixed for 24 h using a Restch planetary ball miller. After milling, the resultant slurry was dried in an oven and then the powders were calcined at 1000 °C for 2 h in a carbolite high-temperature furnace. After being sieved, the calcined powders were subjected to uniaxial pressure of 150 MPa to form pellets. The compacts were then sintered in air at different sintering temperatures (1220–1250 °C) for 20 min in a high-temperature furnace. The heating and cooling rates for all the samples were 5 and 10 °C min^{-1}, respectively.

The density of the sample was measured using the Archimedes method. A JSM scanning electron microscope (SEM) was used to observe the microstructure, from which the grain size of the sample was estimated. For electrical property characterization, both ends of the sample were coated with the ohmic-contacted silver pastes. A KATO X–Y function electrical testing apparatus was used to measure materials resistivity–temperature trajectory, beginning at room temperature (25 °C). A HP 4192A impedance analyser was used to measure materials grain resistivity ranging from 5 to 13 MHz.

4. Results and discussion

The compositional design is a key component to achieve the desired material electrical properties. In the present work, Y_2O_3 and Nb_2O_5, which are the commonly used donors individually [9, 10], were added simultaneously as the double donors to reduce the room-temperature resistivity [11]. The Y^{3+} and Nb^{5+} ions substituted Ba^{2+} and Ti^{4+} ions in the lattices to induce grains semiconductivity. The addition of MnO_2 increased the grain-boundary potential barrier, and enhanced the PTC effect, due to the segregation of Mn at the grain-boundary regions to introduce the surface acceptor states [12]. The additives Al_2O_3, SiO_2, TiO_2 and BN were applied as the sintering aids to lower the sintering temperature [11, 13].

Figure 1 shows the variations of resistivity with measuring temperature for samples sintered at different temperatures. It can be seen that the room-temperature resistivities of the prepared samples are less than 60 Ω cm, and the sample with the lowest resistivity is the one sintered at 1230 °C (30 Ω cm). The resistivity value obtained in the present work is found to be lower, as mentioned in the literature [14–17]. The lower resistivity value measured is attributed to the double donors, $Y_2O_3 + Nb_2O_5$, doped in the material's system. In an earlier work [11], the better effect of double-donor-doping than single-donor-doping on lowering the resistivity of PTC materials has been explained. In summary, the reactions for making grains semiconductive, which are believed to be the key processes for reducing the resistivity in double-donor-doped materials, proceed more completely and thoroughly compared to those doped by single donor. With respect to figure 1, it can be seen that all the samples exhibit the PTC effect in the investigated sintering temperature range. The Curie temperature observed is 90 °C for the samples sintered at 1220, 1230 and 1240 °C, and 100 °C for the sample sintered at 1250 °C. The shift of the Curie temperature of the 1250 °C sintered sample could be attributed to its relatively large grain size, which will be discussed later in the microstructure effect on electrical properties. It is also noted that the resistivity jump (ρ_{max}/ρ_{min}) of the sample decreases with the increase of the sintering temperature. The sample sintered at 1220 °C

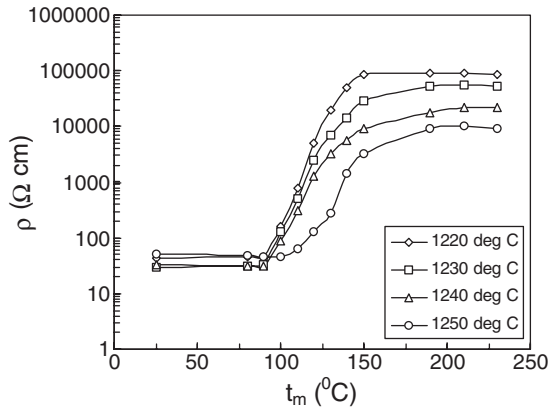

Figure 1. Variations of resistivity with measuring temperature of the samples sintered at different temperatures.

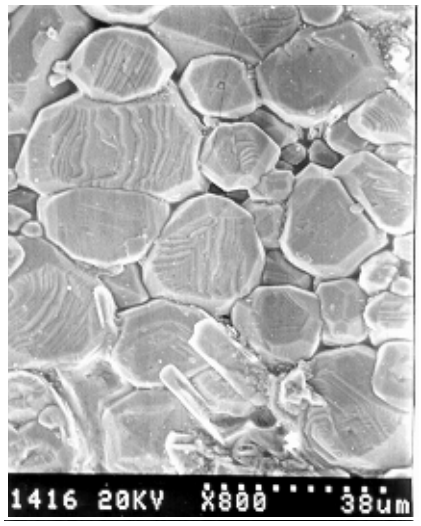

Figure 2. SEM image of the sample sintered at 1230 °C.

achieved the highest value of 2000, and a value of 1800 for the sample sintered at 1230 °C, which possesses the lowest room-temperature resistivity.

For PTC ceramics, the electrical properties have a close relationship with material microstructures. Sintering temperature is one of the most important factors to achieve good microstructure and hence good property. It was reported that high density and moderate grain size could lead to good electrical properties [14, 18]. The SEM image of the sample sintered at 1230 °C is shown in figure 2, which is an illustration to show the microstructure, and the grain size was estimated from it. Figure 3 shows the variations of density and grain size with sintering temperature of the prepared samples. It can be seen that the highest density and moderate grain size was obtained at 1230 °C, which also corresponds to the lowest room-temperature resistivity. Sintering at 1220 °C resulted in only a slight decrease in density, but provided the maximum resistivity jump value. As the sintering temperature increases above 1230 °C, the density of the sample decreases; this is attributed to an occurrence of the fast movement of the grain boundary, leaving trapped pores in the grains. At 1250 °C, this effect is more sensitive to give an even lower density. A larger grain size is also observed due to grain growth. With this microstructure, on average each grain has fewer neighbouring grains. As a result, the total current percolation path is longer and determines a higher room-temperature

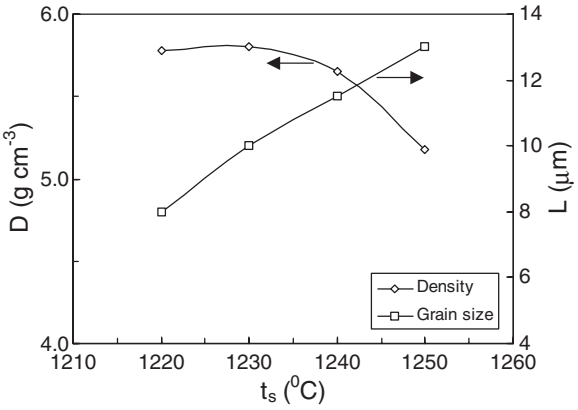

Figure 3. Variations of density and grain size with sintering temperature of the samples.

resistivity. On the other hand, the larger grain size determines a lower number of barriers crossed along the percolation path, as well as a more favourable ratio of intergrain path to depleted boundary region path, which accounts for the smaller jump. As a result, the electrical properties degrade for the sample sintered at 1250 °C, as shown in figure 1. As mentioned earlier, a shift of the Curie temperature was also observed for this sample. It could be attributed to the larger gain size that increases the crystalline constant c/a ratio and hence increases the Curie temperature [19].

From the experimental results obtained, it is noted that, in addition to the compositional design, the electrical properties are also sensitive to the processing conditions. The actual sintering temperature for the present work was selected from 1190 to 1260 °C. The sintered components showed relativity low room-temperature resistivities in the range of 1220–1250 °C, as reported. At other sintering temperatures, the prepared samples exhibited high room-temperature resistivities. The room-temperature resistivities are 102.8 and 120.6 Ω cm for the samples sintered at 1210 and 1260 °C, and furthermore, the room-temperature resistivity value is greater than 10^6 Ω cm for the samples sintered at 1190 and 1200 °C. Therefore, the sintering temperature range is relatively narrow for the materials to achieve desired properties.

The electrical properties investigated thus far are actually the extrinsic parameters. The materials behaviour would be understood more incisively if the intrinsic parameters, which reveal the nature, are determined. To further determine the intrinsic parameters of the samples sintered at different temperatures, the models presented in section 2 are employed, together with the experimental data.

From equations (3)–(5), the resistivity can be expressed as

$$\rho = \rho_0 \exp\alpha \exp\left(-\frac{\alpha T_C}{T}\right) = \rho_0' \exp\left(-\frac{\alpha T_C}{T}\right) \tag{6}$$

where

$$\alpha = \frac{e^2 N_s^2}{2\varepsilon_0 k C N_d}. \tag{7}$$

Based on equation (6), the α values of different sintering temperature samples were determined from the slopes of the logarithm of resistivity against the reciprocal of the absolute measuring temperature, as shown in figure 4. With the determined α values listed in table 1, the grain-boundary potential barrier at and above the Curie temperature was evaluated using

$$\phi = \alpha \frac{k}{e}(T - T_C). \tag{8}$$

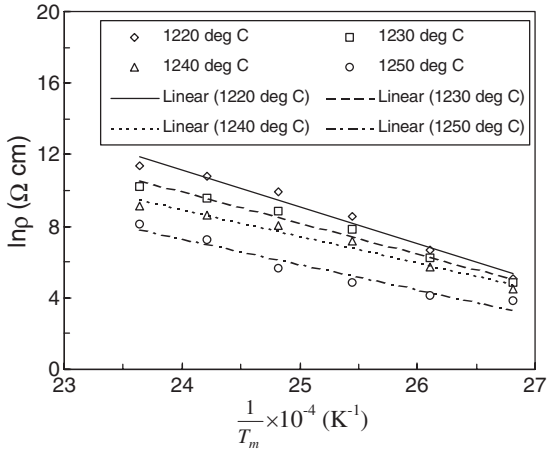

Figure 4. Variations of logarithm of resistivity with the reciprocal of absolute measuring temperature of the samples sintered at different temperatures.

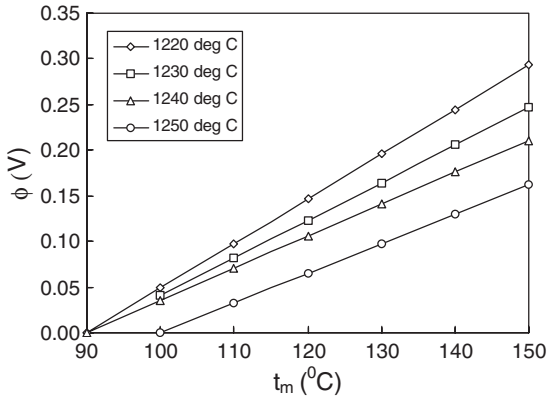

Figure 5. Variations of grain-boundary potential barrier with measuring temperature of the samples sintered at different temperatures.

Table 1. α values evaluated for the samples sintered at different temperatures.

t_s (°C)	1220	1230	1240	1250
α	56.67	47.59	40.74	37.70

Figure 5 shows the variations of the grain-boundary potential barrier with measuring temperature of the samples sintered at different temperatures. It is noted that at a given measuring temperature, the potential barrier decreases as the sample sintering temperature increases. In general, a high potential barrier leads to a high resistivity jump, and hence good PTC effect. This is also consistent with the resistivity–temperature measurement shown in figure 1.

In the present work, the measuring temperature range investigated in figures 4 and 5 corresponds to the working zone, which is the practical working temperature range for the over-current limiter. In the working zone, the sensitivity of the device is high due to the sharp rise of the resistivity with the temperature, compared with the other temperature range. This can also be deduced from figure 1.

With respect to equation (2), the effective donor concentration was calculated. The ρ_b values of the samples sintered at different temperatures were obtained from the impedance spectroscopy measurement, and the mobility was taken as 0.5 cm^2 V^{-1} s^{-1} [20]. With the

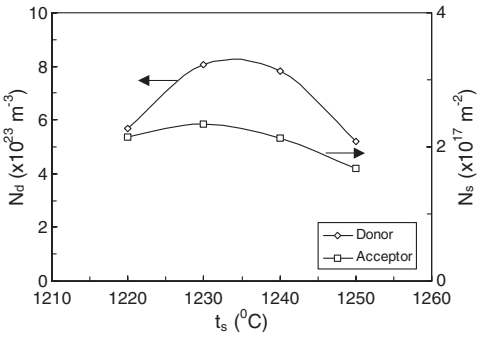

Figure 6. Variations of effective donor concentration and surface acceptor state density with sintering temperature of the samples.

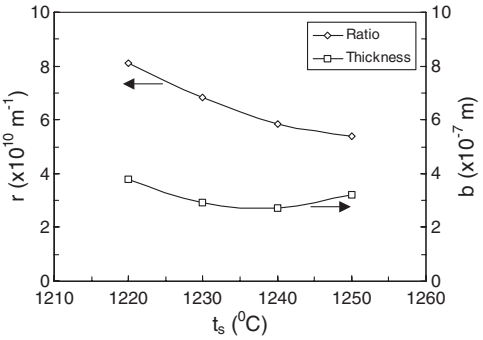

Figure 7. Variations of N_s^2/N_d and depletion layer thickness with sintering temperature of the samples.

calculated N_d and the determined α, the acceptor state density was evaluated from equation (7), with the Curie constant of 1.5×10^5 K [20]. The depletion layer thickness was then obtained using equation (1).

The effective donor concentration and the surface acceptor state density of the samples sintered at different temperatures are shown in figure 6. Similar changes with sintering temperature are seen for both N_d and N_s. They increase and reach the maximum and then drop. It is noted that these two parameters are important in determining the overall electrical properties of PTC materials. The N_d and N_s determined in the present work have the same order of magnitude as reported in the literature [20–22]. In the present work, double donors $Y_2O_3 + Nb_2O_5$ were added in the materials. It is hence noted that the effective donor concentrations of the samples sintered at different temperatures are different, though the originally added donor amount was fixed. Based on the designed composition, the added donor concentration was estimated to be 5×10^{25} m^{-3}. It can be seen that the original donor concentration is much higher than the calculated effective donor concentration. This difference has been reported by Huybrechts *et al* [20], and it is probably caused by partial compensation of the donor charge by vacancies instead of by electrons. The variation of the N_d with sintering temperature could be explained by means of the reactions for making grains semiconductive. As a result, the optimal reaction has been achieved for the sample sintered at 1230 °C, which led to a high N_d. In general, high effective donor concentration results in low room-temperature resistivity, which is consistent with the room-temperature measurement as shown in figure 1. Similar with the relationship between the N_d and the added $Y_2O_3 + Nb_2O_5$, the N_s evaluated is related to the added MnO_2. High surface acceptor state density tends to increase the grain-boundary potential barrier and enhances the resistivity jump and hence the PTC effect. However, the actual resistivity jump depends on the combination of N_d and N_s. Therefore, in the present work, one parameter, r, is introduced,

$$r = \frac{N_s^2}{N_d} \tag{9}$$

which represents more appropriately the resistivity jump. r is actually the product of the depletion layer thickness and the surface acceptor state density, and it is a measure of the potential barrier height and hence the resistivity jump. High r indicates high resistivity jump. Figure 7 shows the variations of r and depletion layer thickness of the samples prepared at different sintering temperatures. It is noted that r decreases with the increase of the sintering temperature, which expresses a consistent trend with the variation of the resistivity jump with

the sintering temperature, as can be seen in figure 1. With respect to figure 7, the depletion layer thicknesses determined are in the submicron range, which are considered as reasonable values when compared with the grain sizes shown in figure 3, which are in the micron range.

5. Conclusions

In the present work, low room-temperature resistivity $(Ba_{0.92}Sr_{0.08})TiO_3$-based PTC ceramics were produced by doping double donors $Y_2O_3 + Nb_2O_5$. The room-temperature resistivity of the sample sintered at 1230 °C is 30 Ω cm. The grain-boundary potential barrier at a fixed measuring temperature decreases with increasing sample sintering temperature. The evaluated effective donor concentration and surface acceptor state density, which are related to the added donors $Y_2O_3 + Nb_2O_5$ and acceptor MnO_2, respectively, are in good agreement with those reported in the literature. One parameter, N_s^2/N_d, is employed to represent the resistivity jump, and both the N_s^2/N_d and the resistivity jump decrease with the increased sintering temperatures of the samples. The depletion layer thickness determined is in the submicron range. The present work is considered to be the first report on the determination of the whole set of intrinsic parameters of double-donor-doped PTC ceramics using experimental data.

References

[1] Heywang W 1964 *J. Am. Ceram. Soc.* **47** 484
[2] Heywang W 1961 *Solid-State Electron.* **3** 51
[3] Jonker G H 1964 *Solid-State Electron.* **7** 895
[4] Daniels J, Hardtl K H and Wernicke R 1978/1979 *Philips Tech. Rev.* **38** 73
[5] Allas A B, Amarakoon R W and Burdick V L 1989 *J. Am. Ceram. Soc.* **72** 148
[6] Chiou B S, Lin S T, Duh J G and Chang P H 1989 *J. Am. Ceram. Soc.* **72** 1967
[7] Haertling G H 1999 *J. Am. Ceram. Soc.* **82** 797
[8] Huang Z Z, Adikary S U, Chan H L W and Choy C L 2002 *J. Mater. Sci.: Mater. Electron.* **13** 221
[9] Ho I C and Hsieh H L 1994 *J. Electron. Mater.* **23** 471
[10] Gillot C, Spira M and Michenaud J P 1993 *Ferroelectrics* **155** 171
[11] He Z, Ma J, Qu Y and Feng X 2002 *J. Eur. Ceram. Soc.* **22** 2143
[12] Illingsworth J, Al-Allak H M, Brinkman A M and Woods J 1990 *J. Appl. Phys.* **67** 2088
[13] Cheng H F 1989 *J. Appl. Phys.* **66** 1382
[14] Lin T F, Hu C T and Lin I N 1990 *J. Am. Ceram. Soc.* **73** 531
[15] Hari N S and Kutty T R N 1998 *J. Mater. Sci.* **33** 3275
[16] Al-shahrani A and Abboudy S 2000 *J. Phys. Chem. Solids* **61** 955
[17] Huang Z Z, Adikary S U and Chan H L W 2002 *J. Mater. Sci.: Mater. Electron.* **13** 605
[18] Osonoi A, Tashiro S and Igarashi H 1997 *Japan. J. Appl. Phys.* **36** 6021
[19] Zhang L, Zhong W L, Wang C L, Zhang P L and Wang Y G 1999 *J. Phys. D: Appl. Phys.* **32** 546
[20] Huybrechts B, Ishizaki K and Takata M 1992 *J. Am. Ceram. Soc.* **75** 722
[21] Chen L F and Tseng T Y 1996 *IEEE Trans. Compon. Packag. Manuf.* A **19** 423
[22] Ho I C and Fu S L 1992 *J. Am. Ceram. Soc.* **75** 728